Draft version September 25, 2006
Preprint typeset using LaTeX style emulateapj v. 05/04/06

IDENTIFICATION OF THE MICROLENS IN EVENT MACHO-LMC-20

Nitya Kallivayalil[1], Brian M. Patten[1], Massimo Marengo[1], Charles Alcock[1], Michael W. Werner[2] and Giovanni G. Fazio[1]

Draft version September 25, 2006

ABSTRACT

We report on the identification of the lens responsible for microlensing event MACHO-LMC-20. As part of a *Spitzer*/IRAC program conducting mid-infrared follow-up of the MACHO Large Magellanic Cloud microlensing fields, we discovered a significant flux excess at the position of the source star for this event. These data, in combination with high resolution near-infrared *Magellan*/PANIC data has allowed us to classify the lens as an early M dwarf in the thick disk of the Milky Way, at a distance of ~ 2 kpc. This is only the second microlens to have been identified, the first also being a M dwarf star in the disk. Together, these two events are still consistent with the expected frequency of nearby stars in the Milky Way thin and thick disks acting as lenses.

Subject headings: Galaxy: structure — gravitational lensing — stars: late-type

1. INTRODUCTION

We have been conducting near and mid-infrared follow-up of the MACHO (Massive Compact Halo Object) Large Magellanic Cloud (LMC) microlensing event fields to try to identify the lensing population. Identification of the lenses can resolve questions regarding their locations, and can support a microlensing interpretation of the events. Deep photometry using *Spitzer's* Infrared Array Camera (IRAC) of all the lensed LMC stars reported by MACHO can be used to test the hypothesis that the Milky Way has a thin or thick disk population of cool stars that are responsible for the lensing.

Such a population would be readily detectable by *Spitzer*, but because IRAC has a spatial resolution of $\sim 1.7''$ (FWHM), not enough time has past since the original microlensing event to allow the source and lens stars to separate via proper motions. However, the presence of a cool lens can be inferred by way of an infrared (IR) excess (Von Hippel et al. 2003). While this technique requires a number of assumptions to be made about the lens and the source star, it has had some success to date. In the case of MACHO-LMC-5 (hereafter Event 5), the lens properties inferred from the flux excess technique using IRAC (Nguyen et al. 2004) were strikingly consistent with those obtained by direct high-resolution *HST* imaging (Alcock et al. 2001b; Gould 2004; Drake et al. 2004). The Event 5 lens was found to be a M5 dwarf in the disk of the Milky Way, and was the only microlens to have been identified to date. On its own it did not shed any light on the microlensing population in general.

In this letter we report the identification of one more lens from the MACHO sample, that for MACHO-LMC-20 (hereafter "Event 20"; Alcock et al. 2000). Event 20 was a low-magnification event ($A_{\rm max} = 2.95$) that occurred in November, 1997. It only passed the looser 'criteria B' MACHO cuts which allowed events of lower signal-to-noise than the stricter 'criteria A' ones (Alcock et al. 2000). The event duration was 72.7 days, which for a typical halo model, places the lens mass at approximately $0.5M_{\odot}$ (Alcock et al. 1993). The baseline (unmagnified) V magnitude of the source+lens system was 21.35, with $V - R = 0.57$. IRAC detected a clear IR excess at the source location in both the 3.6 and 4.5μm bands relative to the expected flux in these bands for a star of the above-mentioned magnitude and color (~ 0.6 mag of excess flux), suggesting blending with a foreground cool star. This data, in combination with subsequent ground-based follow-up using the PANIC infrared imager on Magellan, has enabled us to infer that the lens is an early M dwarf approximately 2 kpc away in the Milky Way thick disk. Together with Event 5, the two events are consistent with the number of events expected from the Milky Way disk, and thus do not signify any anomalous structure in the disk. § 2 briefly describes the IRAC data, § 3 describes the PANIC observations and analysis, and § 4 presents the results and a discussion of them.

2. DESCRIPTION OF SPITZER DATA IN BRIEF

MACHO-LMC-20 (hereafter Event 20) was observed using *Spitzer*/IRAC as part of PID 20121, an ongoing near-IR follow-up investigation of the MACHO LMC fields (follow-up targets are MACHO-LMC-1, 4, 5, 6, 7, 8, 9, 13, 14, 15, 18, 20, 21, 25 & 27). IRAC is a four-channel camera consisting of two pairs of 256×256 pixel InSb and Si:As IBC detectors that provide simultaneous images at 3.6, 4.5, 5.8, and 8μm[3]. Each channel has a field of view of $\sim 5.12' \times 5.12'$ and an $\sim 1.2''$ pixel resolution. As mentioned in the introduction, at this plate-scale, the source and lens star cannot be resolved even for lenses located relatively nearby in the Galactic disk. However, a cool lens would contribute a significant fraction of the source+lens (hereafter designated 'system') emission in the IRAC bandpasses. Note that while we do have to consider how the microlensing system has evolved in time since the peak magnification, the chance

[1] Harvard-Smithsonian Center for Astrophysics, 60 Garden Street, Cambridge, MA 02138
[2] Jet Propulsion Laboratory, California Institute of Technology, 4800 Oak Grove Drive, Pasadena, CA 91107
Electronic address: nkalliva@cfa.harvard.edu

[3] IRAC 3.6 and 4.5μm bands have effective wavelengths similar to the widely used L and M filters respectively (Fazio et al. 2004).

placement of the source star near a foreground red object is very low (see e.g. Alcock et al. 2001b). Thus if the infrared excess coincides with the position of the source star, we are very likely seeing the contribution from a cool lens.

Further results on the IR follow-up will be published in forthcoming papers (see Kallivayalil et al. 2004 & Patten et al. 2005 for a summary of the progress so far). Here we focus on Event 20. The IRAC observations were centered on the event position. The target area was imaged using a 12-position Reuleaux triangle dither pattern with 4 repeat exposures of 30 second FRAMETIME at each position. This strategy produced background-limited images for each individual exposure while the combination of repeats and dithers minimized the impact of cosmic rays, bad pixels and other fixed-pattern noise in the arrays. The total effective exposure time was 1440 seconds in each IRAC band.

The data were reduced using the IRAC post-BCD (basic calibrated data) processing software "IRACproc" (Schuster et al. 2006). In brief, the software mosaics the basic calibrated data delivered by the Spitzer Science Center and performs cosmic ray and bad pixel rejection. The individual frames were visually inspected to ensure that the target area was clean of cosmic rays and other blatant artifacts before processing.

In order to identify the position of the source stars in our IRAC data, we registered the cleaned mosaics with the MACHO R-band discovery images[4]. This was quite straightforward as the MACHO and IRAC pixel scales are comparable. Figure 1 shows the MACHO image of Event 20 on the top panel. The crosshairs are centered on the system. For comparison, the final mosaic of the IRAC 3.6μm data is shown on the bottom with a circle highlighting the system. The IR excess is visible by eye. The APPHOT package in IRAF was used to perform aperture photometry on the cleaned mosaics, and aperture corrections were performed for the source apertures that we employed. Table 1 shows the IRAC 3.6 and 4.5μm (hereafter [3.6] & [4.5]) photometry for the system (which is dominated by the flux of the lens candidate). We had no detections in the two longer IRAC bands.

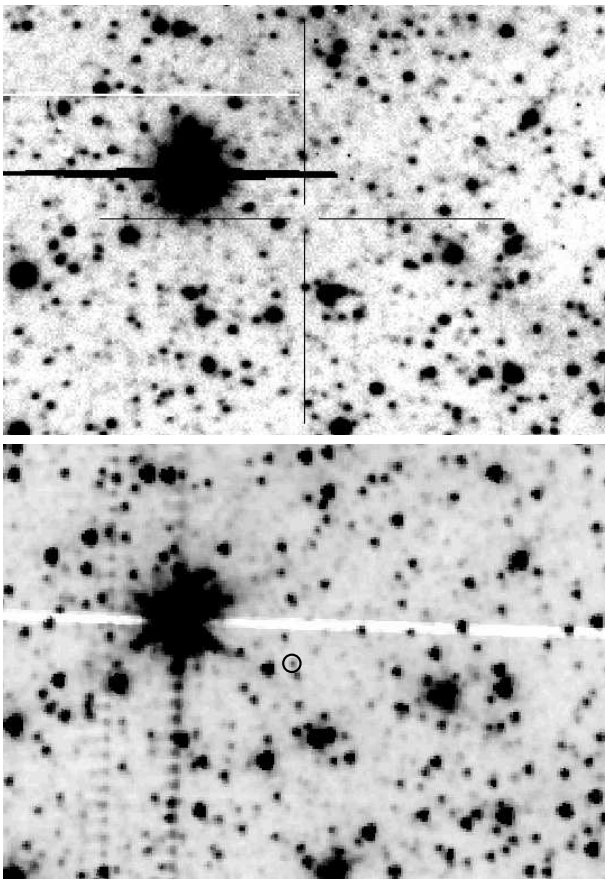

FIG. 1.— (*Top*) The (baseline) R-band MACHO image of Event 20. The crosshairs are centered on the system. (*Bottom*) The IRAC [3.6] image of the same field. The circle highlights the system.

3. DESCRIPTION OF PANIC OBSERVATIONS AND ANALYSIS

With detections only in the first two IRAC bands, we were left with a certain amount of color-degeneracy in determining whether the lens is a M or L-dwarf, or even something more massive (see Patten et al. 2006). To address this problem we secured *Magellan*/PANIC (Persson's Auxiliary Nasmyth Infrared Camera) high resolution J, H and K_s-band imaging in order to characterize the lens. The JHK_s data in combination with IRAC would allow for a clearer discrimination between M and L dwarfs, and the high resolution ($0.125''$ per pixel, $128'' \times 128''$ field-of-view) would allow us to ascertain whether the IR excess was from a point-source like system, as we expected, or from an unrelated neighbor.

We observed the field of Event 20 for most of the night on January 10, 2006. The source star is faint (see Table 1) and we had to integrate on source for 45 minutes (60 second frames) in J-band, 50 minutes (15 second frames) in H-band and 50 minutes (15 second frames) in K_s-band in order to achieve S/N$>$ 10 in all bands. The use of a $5'' \times 5''$ step dither also allowed us to observe the target star and reference stars at different places in the pixel grid. The viewing conditions were non-photometric, with the seeing changing from $0.7''$ to $0.4''$ and back up to $0.5''$ over the course of the night. We took repeated observations of 9 bright 2MASS (Skrutskie et al. 2006) comparison stars distributed around the Event 20 field in order to get a good handle on how the sky was varying over the night, and thus our systematic errors, and also to tie all the photometry down to the 2MASS system. The 9 2MASS stars were distributed in 3 fields, which we call fields A, B & C for future reference.

The data were reduced using the GOPANIC routine in the PANIC IRAF software (Martini et al. 2004). The GOPANIC task provides a complete pipeline for PANIC data, including summing the images in a loop, applying a linearity correction, flat-fielding, sky subtraction and distortion correction. The final images showed that the system is still a point source, with no evidence of a displacement of the IR source from the MACHO position. The DAOPHOT package in IRAF (Stetson 1987) was used to fit an empirical point spread function (PSF) to the final images and to do photometry.

Our analysis strategy was simply to calculate a magnitude offset (essentially a zero point) between the magnitudes that we measured for the comparison stars in each

[4] The finder charts for the MACHO LMC events are available at http://wwwmacho.mcmaster.ca/.

of our fields and the known 2MASS magnitudes, and then to use this offset in order to calibrate the photometry of the lens candidate. One component of the final photometric error would thus be the RMS of these field offsets, since in photometric conditions, the offsets should all be the same (modulo any variability in the 2MASS stars). Since conditions were not photometric however, in addition to the zero-point offset we also needed to calculate an additional field-dependent offset, which would tie the 3 standard fields and the Event 20 field together. This was done using the common stars in the fields. Fields A & B had regions of overlap with the Event 20 field and could thus be directly tied to it. Field C overlapped with field B, and was tied to the field of Event 20 via field B. Our final offset per field, Δm(field), was then calculated from the 2MASS offset, $\Delta m_{\rm 2MASS}$, and the field-dependent calibration term, *calib*(field), simply as follows:

$$\Delta m(\text{field}) = \Delta m_{\rm 2MASS} + calib(\text{field}). \quad (1)$$

The *calib*(field) terms were typically small, consistent with photometric variations caused by changes in the seeing. They were estimated from roughly 10 common stars in each overlap region. Once we had an estimate of Δm(field) from fields A, B & C, we calculated a mean value that could be applied to our photometry for the lens candidate. The RMS of Δm(field) is a direct measure of both random and systematic photometric errors. We calculated our final photometric error for each filter as the quadrature sum of the photometric error of the lens candidate, and the RMS of the Δm(field)s. The typical final error is ~ 0.05 mag. Given these errors we did not think it necessary to implement any higher order corrections to our calibration, such as color terms. The PANIC photometry of the lens is presented in Table 1.

4. RESULTS & DISCUSSION

The suggestion of microlensing by the Galactic dark halo (Paczynski 1986) was followed-up by many teams. While the MACHO collaboration reported 16 microlensing events towards the LMC (Alcock et al. 1993, 1997, 2000), the EROS collaboration has found only 3 (Aubourg et al. 1993; Lasserre et al. 2000). The MACHO efficiency analysis indicates a dark halo with a MACHO fraction of 20% which corresponds to an optical depth of $\tau = 1.2^{+0.4}_{-0.3} \times 10^{-7}$ due to lenses of $\sim 0.5 M_\odot$. This rate is *significantly* higher than what was expected from known Galactic and LMC stellar populations; the latter have τ between 0.24×10^{-7} and 0.36×10^{-7} (Alcock et al. 2000; Griest & Thomas 2005). The upper limit on the EROS microlensing optical depth is only barely consistent with that of MACHO. Recently, the EROS-2 project reported their results, and combined with the results of EROS-1, they report an optical depth toward the LMC of $\tau < 0.36 \times 10^{-7}$ (95% confidence) due to lenses of $\sim 0.4 M_\odot$, corresponding to a halo mass fraction of less than 7% (Tisserand et al. 2006).

Several groups have investigated the excess of microlensing towards the LMC seen by MACHO, attributing it to as yet undetected structure in the Milky Way (Rahvar 2005; Nguyen et al. 2004; Gates & Gyuk 2001; Evans et al. 1998; Zhao 1998; Zaritsky & Lin 1997) or in the LMC itself (Wu 1994, Sahu 1994; Alves & Nelson 2000; Evans & Kerins 2000; Di Stefano 2000; Gyuk et al. 2000; Zhao et al. 2003; Mancini et al. 2004; Alves 2004; Nikolaev et al. 2004). However, over and above the question of the population responsible for the lensing, the discrepancy between the MACHO and EROS results have also cast doubt on whether the MACHO events are microlensing at all, or just contamination from variable stars and background supernovae. Belokurov et al. (2003, 2004) applied a neural network analysis to the MACHO data in an attempt to develop independent selection criteria for microlensing. They selected only 10 of the candidates that MACHO picked out as bona fide microlensing. Their verdict on the microlensing events as well as the original MACHO verdict are presented in Table 4 of Bennett et al. (2005).

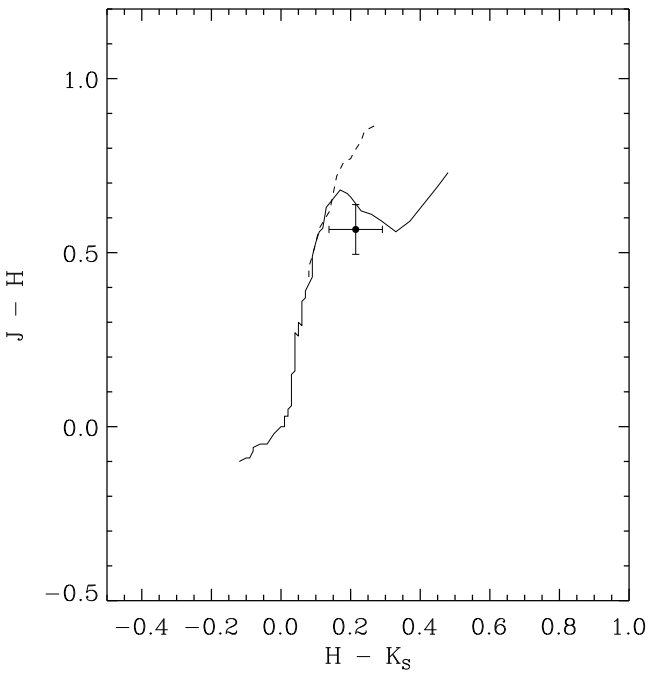

FIG. 2.— A plot in $J-H$ vs. $H-K_s$–space showing the intrinsic relation for dwarfs (solid line) and giants (dashed line). The filled circle with error bars shows our PANIC photometry for the Event 20 system.

In the case of the event at hand, Belokurov et al. (2003) used their neural network to classify it as a supernova (SN) rather than microlensing. However, Bennett et al. (2005) pointed out that Event 20 is a good disk lens candidate because Figure 7 of Alcock et al. (2000) shows that, like Event 5, Event 20 is quite red for its brightness, i.e. it appears to be blended with a star that is much redder than other LMC stars of similar magnitude.

Our data allows us to weigh into this debate. Figure 2 is a $J-H$ vs. $H-K_s$ plot, showing the intrinsic relation for dwarfs (solid line) and giants (dashed line; dwarf data from Leggett 1992 and Kenyon & Hartmann 1995; giant data from Bessell & Brett 1988) . The filled circle with error bars shows our PANIC result for the lens, which appears to be consistent with an early-M dwarf star. The mean extinction at the location of Event 20 in the LMC is $A_V \sim 0.5$ mag (Zaritsky et al. 2004). This implies that, even if our M dwarf is at the distance of the LMC (in which case we certainly would not see it with

TABLE 1
Photometry for Event 20

MACHO ID	17.2221.1574
RA, DEC (2000)	04 54 19, -70 02 15
V	21.35
J	18.84 ± 0.04
H	18.28 ± 0.06
K_s	18.06 ± 0.05
[3.6]	18.02 ± 0.11
[4.5]	18.37 ± 0.21

Note. — The data for the first three rows are from Alcock et al. 2000.

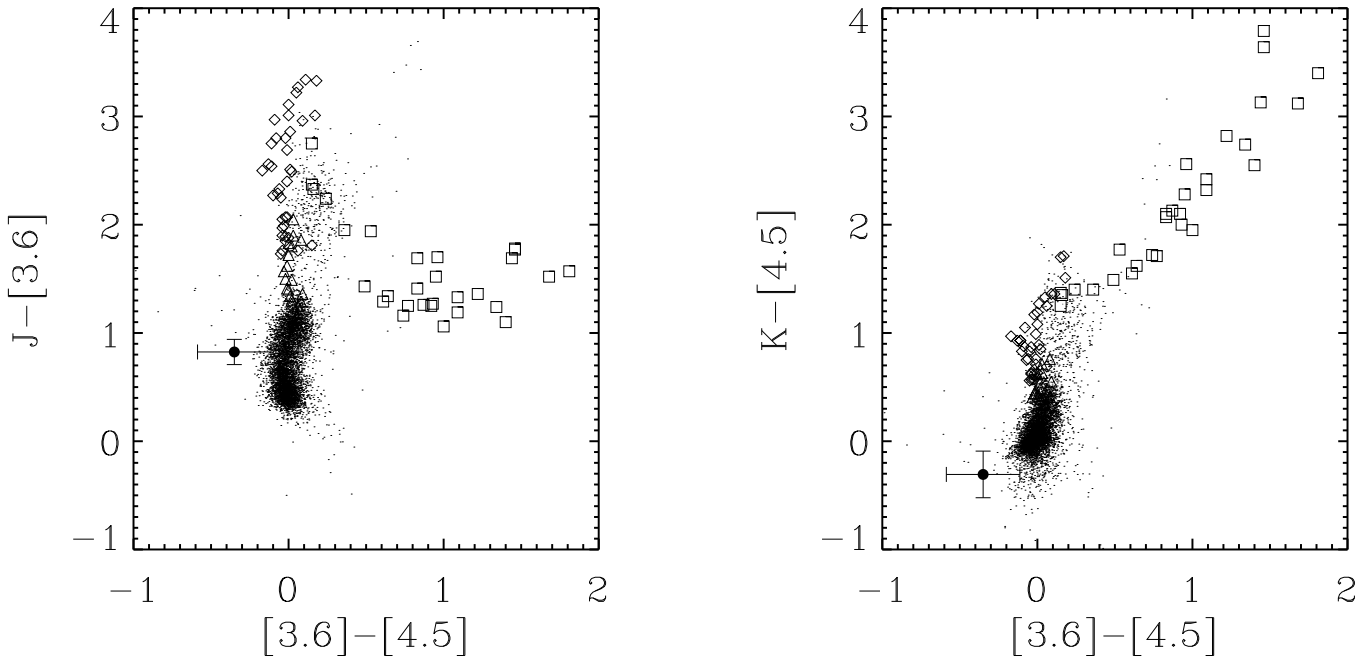

Fig. 3.— (*Left*) A plot showing $J-[3.6]$ vs. $[3.6]-[4.5]$ for stars and galaxies in the First Look Survey. Late-type M dwarfs from the Patten et al. (2006) sample are overlaid using triangles, L dwarfs using diamonds and T dwarfs using squares. The filled circle with error bars shows are PANIC+IRAC photometry for the Event 20 system. (*Right*) The same objects are shown in $K-[4.5]$ vs. $[3.6]-[4.5]$-space

either PANIC or IRAC), the mean extinction in K-band would be $A_K \sim 0.05$. This is within our photometric errors, and thus we do not account for reddening. Note, however, that in this and all following analysis plots, the lens object is still blended with the LMC source star. At these infrared wavelengths we expect that the contamination from the source flux is minimal ($\sim 10\%$). The data thus seem to corroborate Bennett's prediction of this event has lensing by a low-mass star.

However, as suggested by Belokurov et al. (2003), we also consider the possibility that the magnification in the MACHO light curve was caused by a background SN. If this were the case, at ~ 9 years since the event we would now be seeing the host galaxy. In Figure 3 we address this by showing the near-IR color-color space of objects in the *Spitzer*/IRAC First Look Survey (Lacy et al. 2005) for which 2MASS J and K photometry is available. The panel on the left shows $J-[3.6]$ vs. $[3.6]-[4.5]$. The points are stars and galaxies, with the blue end of the plot comprising mostly main sequence stars. The galaxies tend to be redder and extend into the diffuse plume at the red end of the y-axis. Overlaid are late-M dwarfs (spectral type M6 and later) (triangles), L dwarfs (diamonds) and T-dwarfs (squares) from Patten et al. (2006). The filled circle with error bars shows the IRAC+ PANIC photometry for the lens. The lens lies in a part of the color-color space that is more consistent with stars than with galaxies, and within the large errors propagated through from the IRAC photometry, it is consistent with an early M dwarf. The panel on the right shows $K-[4.5]$ vs. $[3.6]-[4.5]$. Again, the points at the blue end of the plot are mostly stars with galaxies extending into a red tail. In this color-space as well the data suggest that the lens is a M dwarf and not a background galaxy. The placement of the lens could be consistent with a blue galaxy, however, at the JHK_s magnitude of the lens, we

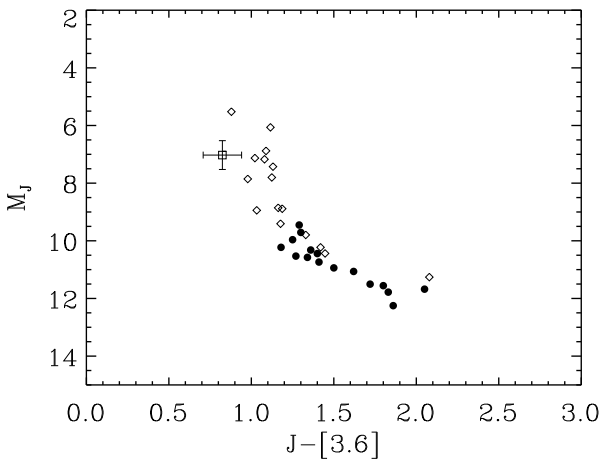

FIG. 4.— A plot showing M_J vs. $J-[3.6]$ for M dwarfs (and 2 K7 dwarfs) from the Patten et al. (2006) sample (filled circles), and some earlier type M dwarfs from M. Schuster (private communication) (diamonds). The square with error bars shows the lens candidate, which is consistent with where early M dwarfs lie on this relation.

would expect that galaxies are discernible from stars in the high resolution PANIC images.

Thus our follow-up data confirm not only the microlensing nature of this event but also that it was caused by a low-mass star. Finally, Mancini et al. (2004) have made predictions, based on detailed models of the LMC, about which of the MACHO events were likely due to lenses in the LMC itself. They picked events 6, 8, 13 & 14 as most likely due to self-lensing because of their locations in the LMC. Event 20 was not picked as a high probability self-lensing candidate. The Mancini et al. (2004) predictions are tabulated and compared against the MACHO and Belokurov et al. (2004) predictions in Bennett et al. (2005).

Given our measurement of the spectral type of the lens, we estimate its distance from a sample of early M dwarfs using 2MASS JHK_s and [3.6] photometry provided by M. Schuster (private communication). If the M dwarf is in the range M0–3.5, then its absolute magnitude would be in the range $M_J = 7 \pm 0.5, M_H = 7 \pm 0.5, M_{K_s} = 6 \pm 0.4$, and $M_{[3.6]} = 6 \pm 0.3$. In addition to this line of argument, in Figure 4 we show M_J versus J-[3.6] for these M dwarfs (plus two K7 dwarfs and additional late-type M dwarfs from M. Schuster) (triangles) and for some late-type M dwarfs from Patten et al. (2006) (filled circles). The square with error bars is the lens and it is clear that its J-[3.6] color is consistent with the absolute magnitude expected for an early M dwarf ($M_J \sim 7$). The range of absolute magnitudes quoted above imply a distance to the lens of 2 ± 0.7 kpc where the error includes contributions from the range in spectral types and the photometric error in the J-[3.6] color. The lens is thus in the thick disk of the Milky Way[5]. This is the second Milky Way disk lens in the MACHO sample, the first being that of Event 5, which was closer at ~ 600 pc. A total of 0.75 events were expected from the Milky Way thin and thick disks (Bennett et al. 2005), and thus these two disk lenses are still consistent with the expected number. Event 20 did not pass the MACHO criteria set 'A' and so does not affect the conclusion to the halo fraction made from it.

In a future paper we will present the full consensus of the near-IR follow-up of the MACHO LMC microlensing fields. The main result of this project thus far is that two of the microlensing events were caused by foreground disk lenses. This is consistent with what was expected from the Milky Way thin and thick disks.

The authors would like to thank M. Schuster for providing IRAC photometry of some nearby M dwarfs. This work is based [in part] on observations made with the Spitzer Space Telescope, which is operated by the Jet Propulsion Laboratory, California Institute of Technology under a contract with NASA. Support for this work was provided by NASA through an award issued by JPL/Caltech. This publication also makes use of data products from the Two Micron All Sky Survey, which is a joint project of the University of Massachusetts and the Infrared Processing and Analysis Center/California Institute of Technology, funded by the National Aeronautics and Space Administration and the National Science Foundation, and the SIMBAD database, operated at CDS, Strasbourg, France.

Facilities: Magellan:Baade (PANIC), Spitzer (IRAC)

[5] Events 20 & 5 are evidence that nearby dim stars can be studied through such monitoring programs ("mesolensing", Di Stefano 2005).

REFERENCES

Afonso, C., et al. 2003, A&A, 400, 951
Alcock, C., et al. 1993, Nature, 365, 621
Alcock, C., et al. 1997, ApJ, 486, 697
Alcock, C., et al. 2000, ApJ, 542, 281
Alcock, C., et al. 2001a, ApJ, 552, 582
Alcock, C., et al. 2001b, Nature, 414, 617
Aubourg, E., et al. 1993, Nature, 365, 623
Alves, D. R. 2004, ApJ, 601, L151
Alves, D. R. & Nelson, C. A. 2000, ApJ, 542, 789
Belokurov, V., Evans, N. W., & Du, Y. L. 2003, MNRAS, 341, 1373
Belokurov, V., Evans, N. W., & Le Du, Y. 2004, MNRAS, 352, 233
Bennett, D. P., Becker, A. C., & Tomaney, A. 2005, ApJ, 631, 301
Bessell, M. S., & Brett, J. M. 1988, PASP, 100, 1134
Di Stefano, R. 2000, ApJ, 541, 587
Di Stefano, R. 2005, ApJ submitted, astro-ph/0511633
Drake, A. J., Cook, K. H., & Keller, S. C. 2004, ApJ, 607, L29
Evans, N. W., Gyuk, G., Turner, M. S., & Binney, J. 1998, ApJ, 501, L45
Evans, N. W., & Kerins, E. 2000, ApJ, 529, 917
Fazio, G. G., et al. 2004, ApJS, 154, 10
Gates, E. I. & Gyuk, G. 2001, ApJ, 547, 786
Gould, A. 2004, ApJ, 606, 319
Griest, K., & Thomas, C. L. 2005, MNRAS, 359, 464
Gyuk, G., Dalal, N., & Griest, K. 2000, ApJ, 535, 90
Kallivayalil, N., Patten, B. M., Alcock, C., Nguyen, H. T., & Werner, M. W. 2004, Bulletin of the American Astronomical Society, 36, 1391
Kenyon, S. J., & Hartmann, L. 1995, ApJS, 101, 117
Lacy, M., et al. 2005, ApJS, 161, 41
Lasserre, T., et al. 2000, A&A, 355, L39
Leggett, S. J. 1992, ApJS, 82, 351
Mancini, L., Calchi Novati, S., Jetzer, P., & Scarpetta, G. 2004, A&A, 427, 61

Martini, P., Persson, S. E., Murphy, D. C., Birk, C., Shectman, S. A., Gunnels, S. M., & Koch, E. 2004, Proc. SPIE, 5492, 1653
Nikolaev, S., Drake, A. J., Keller, S. C., Cook, K. H., Dalal, N., Griest, K., Welch, D. L., & Kanbur, S. M. 2004, ApJ, 601, 260
Nguyen, H. T., Kallivayalil, N., Werner, M. W., Alcock, C., Patten, B. M., & Stern, D. 2004, ApJS, 154, 266
Paczynski, B. 1986, ApJ, 304, 1
Patten, B. M., Kallivayalil, N., Alcock, C., Werner, M. W., & Fazio, G. G. 2005, Bulletin of the American Astronomical Society, 37, 1400
Patten, B. M. et al. 2006, ApJ accepted, astro-ph/0606432
Rahvar, S. 2005, MNRAS, 356, 1127
Sahu, K. C. 1994, Nature, 370, 275
Schuster M. T., Marengo, M. & Patten, B. M., 2006, Astronomical Telescopes and Instrumentation, Proc. SPIE, 6270
Skrutskie, M. F., et al. 2006, AJ, 131, 1163
Stetson, P. B. 1987, PASP, 99, 191
Tisserand et al. 2006, A&A submitted, astro-ph/0607207
Von Hippel, T., Sarajedini, A., & Ruiz, M. T. 2003, ApJ, 595, 794
Wu, X.-P. 1994, ApJ, 435, 66
Zaritsky, D. & Lin, D. N. C. 1997, AJ, 114, 2545
Zaritsky, D., Harris, J., Thompson, I. B., & Grebel, E. K. 2004, AJ, 128, 1606
Zhao, H. 1998, MNRAS, 294, 139
Zhao, H., Ibata, R. A., Lewis, G. F., & Irwin, M. J. 2003, MNRAS, 339, 701